A 20 m.y. long-lived successive mineralization in the giant Dahutang W–Cu–Mo deposit, South China

Article *in* Ore Geology Reviews · February 2018

DOI: 10.1016/j.oregeorev.2018.02.033

CITATIONS
4

READS
118

8 authors, including:

Weile Song
Chinese Academy of Sciences
4 PUBLICATIONS **21** CITATIONS
SEE PROFILE

Jun-Ming Yao
Chinese Academy of Sciences
56 PUBLICATIONS **1,052** CITATIONS
SEE PROFILE

Weidong Sun
Institute of Oceanology
391 PUBLICATIONS **22,771** CITATIONS
SEE PROFILE

Kit Lai
Universiti Brunei Darussalam
50 PUBLICATIONS **709** CITATIONS
SEE PROFILE

Ore Geology Reviews 95 (2018) 401–407

Contents lists available at ScienceDirect

Ore Geology Reviews

journal homepage: www.elsevier.com/locate/oregeorev

A 20 m.y. long-lived successive mineralization in the giant Dahutang W–Cu–Mo deposit, South China

Weile Song[a,b], Junming Yao[a,*], Huayong Chen[a], Weidong Sun[a,c], Chunkit Lai[d,e], Xinkui Xiang[f], Xiaohong Luo[g], Fred Jourdan[h]

[a] Key Laboratory of Mineralogy and Metallogeny, Guangzhou Institute of Geochemistry, Chinese Academy of Sciences, 511 Kehua Street, Wushan, Guangzhou 510640, China
[b] University of Chinese Academy of Sciences, No. 19 Yuquan Road, Beijing 100049, China
[c] Center of Deep Sea Research, Institute of Oceanology, Chinese Academy of Sciences, 7 Nanhai Road, Qingdao 266071, China
[d] Faculty of Science, University Brunei Darussalam, Gadong BE1410, Brunei Darussalam
[e] ARC Center of Excellence in Ore Deposits (CODES), University of Tasmania, Hobart, Tasmania 7001, Australia
[f] No. 916 Geological Team, Jiangxi Bureau of Geology, Mineral Resources, Exploration and Development, Jiujiang 332000, China
[g] Northwestern Geological Team, Jiangxi Bureau of Geology, Mineral Resources, Exploration and Development, Jiujiang 332100, China
[h] Western Australian Argon Isotope Facility, Department of Applied Geology & JdL-CMS, Curtin University, GPO Box U1987, Perth, WA 6845, Australia

ARTICLE INFO

Keywords:
Dahutang W–Cu–Mo deposit
Mesozoic magmatism
Successive mineralization
South China

ABSTRACT

The connection between prolonged granitic magmatism and the formation of giant tungsten (W) polymetallic deposits has long been disputed. In this study, we present 6 mica Ar–Ar plateau ages and 22 molybdenite Re–Os model ages data on the newly discovered giant Dahutang W–Cu–Mo deposit in South China, which is one of the largest W deposits in the world. New and published zircon U–Pb, mica Ar–Ar, and molybdenite Re–Os age data reveal that the Mesozoic Dahutang magmatism and mineralization occurred in two major periods: (1) the Late Jurassic (ca. 153–147 Ma), forming the hydrothermal breccia, large wolframite-bearing quartz vein, and scheelite-dominated disseminated/veinlet type orebodies, which is mainly associated with the emplacement of porphyritic biotite granite; (2) the Late Jurassic to Early Cretaceous (ca. 146–130 Ma), forming the Cu–Mo–W ± Sn mineralization overprinting the Late Jurassic W–Mo ± Cu orebodies, which is mainly related to the successively emplacement of the Early Cretaceous granites. We suggest that continuous accumulation of mineralization for a long period of time (151–130 Ma) have contributed to the formation of the giant Dahutang deposit.

1. Introduction

The possible correlation between the duration of magmatism and the size of hydrothermal deposits has been a long and controversial topic, especially when super-large/giant-scale mineralization is concerned (Cathles et al., 1997; Mercer et al., 2015; Buret et al., 2016; Rezeau et al., 2016). What is often neglected in these discussions is the accurate occurrence of multi-stage magmatism and mineralization, which can substantially enlarge and enrich the ore deposits.

The recently discovered Dahutang W–Cu–Mo deposit in South China is a giant deposit, hosting an estimated resource of up to 1.1 million tonnes (Mt) of WO_3, 0.65 Mt Cu and 0.08 Mt Mo (Mao et al., 2013; Zhang et al., 2014; Jiang et al., 2015). Dating of the ore-forming granites yielded a very wide age range from ca. 151.7 Ma–130.3 Ma (Huang and Jiang, 2012, 2013, 2014; Xiang et al., 2012; Mao et al., 2015; Ye et al., 2016; Zhang et al., 2016), while the mineralization ages reported mainly cluster around 150 Ma (Xiang et al., 2013; Zhang et al., 2016), 143 Ma (Feng et al., 2012; Jiang et al., 2015) and 139 Ma (Mao et al., 2013; Zhang et al., 2017). How the wide magmatic age range and the seemingly discrete mineralization episodes are related is poorly understood, which leads to different interpretations of the ore-forming processes. In this contribution, based on detailed documentation of the mineral assemblages and alteration/mineralization paragenesis, we have identified four distinct magmatic-metallogenic phases at Dahutang. Timing of these four magmatic-metallogenic phases is newly constrained by our new molybdenite Re–Os and mica Ar–Ar dating, augmented by the published radiometric ages. We propose that the prolonged and multi-stage magmatism/mineralization has contributed to the giant-scale mineralization at Dahutang.

* Corresponding author.
E-mail address: yaojunming@gig.ac.cn (J. Yao).

https://doi.org/10.1016/j.oregeorev.2018.02.033
Received 2 December 2017; Received in revised form 20 February 2018; Accepted 26 February 2018
Available online 27 February 2018

2. Regional and deposit geology

South China has long been recognized as one of the world's major W mineral provinces (Hsu, 1943), boasting a resource of over 5.6 Mt of WO_3 (Shen et al., 2015; USGS, 2017). The newly discovered Dahutang W–Cu–Mo deposit comprises the North Dahutang, Central Dahutang and South Dahutang ore blocks (Supplementary Fig. A.1). At Dahutang, the low-grade metamorphic rocks of the Neoproterozoic Shuangqiaoshan Group were intruded by the Neoproterozoic Jiuling biotite granodiorite (zircon U–Pb age: 819 ± 9 Ma, Li et al., 2003). Multiple phases of Late Mesozoic granitic intrusions, closely mineralization-related, were emplaced as stocks and dikes into the Neoproterozoic granodiorite and Neoproterozoic Shuangqiaoshan Group metamorphic rocks. Field geological and petrographic observations suggest that the Late Mesozoic granites consist of porphyritic biotite granite (G1), fine-grained biotite granite (G2), porphyritic muscovite granite (G3), granite porphyry (G4), fine-grained muscovite granite (G5), granite porphyry (G6), medium- to fine-grained muscovite granite (G7), porphyritic two-mica granite (G8), and fine-grained two-mica granite (G9).

The W–Cu–Mo mineralization at Dahutang mainly occurs around the intrusive contacts of the Late Mesozoic granite stocks. Major ore types include disseminated/veinlets, large wolframite-bearing-quartz veins, and hydrothermal breccias. Previous field observations and molybdenite Re–Os dating suggest no discernible spatial or temporal relationships among the three types of mineralization. Ore minerals at Dahutang include mainly scheelite, wolframite, chalcopyrite, and molybdenite, with minor cassiterite, sphalerite, bornite, arsenopyrite, pyrite, and stannite. Gangue minerals at Dahutang include predominately quartz, with minor mica, feldspar, fluorapatite, fluorite, chlorite, and calcite.

3. Analytical methods

3.1. Mica $^{40}Ar/^{39}Ar$ dating

Five muscovite and one biotite samples for $^{40}Ar/^{39}Ar$ dating were collected from drill cores and underground tunnels of the Central and South Dahutang ore blocks. Locations and descriptions of these samples are given in Supplementary Table B1. One biotite (DH-31) and two muscovite samples (DH-42, DH-126) were conducted at the Key Laboratory of Orogenic Belts and Crustal Evolution, Peking University, the other three muscovite samples (DH-02, DH-120 and DH-94) were performed at the Western Australian Argon Isotope Facility of Curtin University. The $^{40}Ar/^{39}Ar$ analytical methods as follows:

$^{40}Ar/^{39}Ar$ analytical method at Curtin University: The samples were crushed to 0.10–0.20 mm size fraction. The muscovite was carefully handpicked under a binocular microscope, and then washed in an ultrasonic bath using ultrapure water. Purity of the mineral separates exceeds 99%. The selected muscovite grains were loaded into a small aluminum disc (1.9 cm in diameter, 0.3 cm deep), which was Cd-shielded to minimize nuclear interference reactions. The samples were irradiated for 40 h in the US Geological Survey nuclear reactor (Denver, USA) in central position over two irradiations. The $^{40}Ar/^{39}Ar$ analysis was performed at the Western Australian Argon Isotope Facility of Curtin University. The samples were step-heated using the 110 W Spectron Laser Systems, with a continuous Nd-YAG (IR; 1064 nm) laser rastered over the sample during 1 min to ensure a homogenously distributed temperature. The gas was purified in a stainless steel extraction line using three SAES AP10 getters and a liquid nitrogen condensation trap. Argon isotopes were measured in the static mode using a MAP 215-50 mass spectrometer (resolution: ~500; sensitivity: 4×10^{-14}). The age was calculated using the recommended Fish Canyon sanidine (FCs) age (28.294 ± 0.037 Ma; Jourdan and Renne, 2007; Merle et al., 2009). Mean J-value computed from the monitor mineral is 0.01055080 ± 0.00000422. The correction factors for interfering isotopes were $(^{39}Ar/^{37}Ar)_{ca} = 7.6 \times 10^{-4}$ (± 12%), $(^{36}Ar/^{37}Ar)_{ca} = 2.3 \times 10^{-4}$ (± 1%), $(^{40}Ar/^{39}Ar)_{k} = 7.3 \times 10^{-4}$ (± 13%). Our criteria for the plateau determination are as follows: The plateaus must include at least 70% of ^{39}Ar. The plateau should also be distributed over a minimum of three consecutive steps agreeing at 95% confidence level, and satisfying a probability of fit of at least 0.05. Plateau ages are given at the 2σ level and are calculated using the mean of all the plateau steps, each weighted by the inverse variance of their individual analytical error.

$^{40}Ar/^{39}Ar$ analytical method at Peking University: The samples were crushed to 0.18–0.28 mm size fraction. About 20–60 mg muscovite or biotite was packed in pure aluminous foil for each sample. The foils were placed in evacuated quartz tubes and irradiated in position B4 of 49-2 Nuclear Reactor at the Institute of Chinese Atomic Energy for 24 h, with an irradiation flux of 2.65×10^{13} fast neutrons/cm^2. Neutron flux variation (J) was measured using the standard mineral Zhoukoudian biotite (ZBH-25; 132.7 Ma). After irradiation, the samples were heated to total fusion in a tantalum furnace, during 10–16 stepwise-heating stages. Extracted gas was analyzed using a RGA10 mass spectrometer at the Key Laboratory of Orogenic Belts and Crustal Evolution, Peking University. Argon isotope data were corrected for system blanks, mass discrimination, and interfering neutron reactions with Ca and K. Correction factors are: $(^{36}Ar/^{37}Ar)_{Ca} = 0.000271$, $(^{39}Ar/^{37}Ar)_{Ca} = 0.000652$, and $(^{40}Ar/^{39}Ar)_{K} = 0.00703$. The analyzed argon isotope data were corrected using the $^{40}Ar/^{39}Ar$ Dating 1.2 software developed by the Key Laboratory of Orogenic Belts and Crustal Evolution, Peking University. Plateau and isochron ages were calculated using the Isoplot 3.0 software of Ludwig (2003).

3.2. Molybdenite Re–Os dating

Twenty-two molybdenite samples for the Re–Os dating have been systematically collected from drill cores and underground tunnels of the North, Central and South Dahutang ore blocks. Sampling locations/depths and mineralogical features of the samples are summarized in Supplementary Table B.2.

Molybdenite grains were magnetically separated and then hand-picked under a binocular microscope to obtain a > 99% purity. Re–Os isotope analyses were conducted at the Key Laboratory of Mineralogy and Metallogeny, Guangzhou Institute of Geochemistry, Chinese Academy of Sciences (GIGCAS). The Carius tube method was used for the dissolution of molybdenite and equilibration of samples, and tracer ^{185}Re and ^{190}Os at 225–230 °C for 24 h (Sun et al., 2001, 2010; Li et al., 2011; Leng et al., 2012). From the opened tube, an approximate amount of the supernatant was transferred to a 30 ml quartz beaker, heated to dryness at 150 °C, and then 0.5 ml HNO_3 was added and dried-down. This step was repeated twice to ensure the removal of Os as OsO_4, and finally diluted to 10 ml (using 2% HNO_3) for the Re isotope analysis by ICP–MS. The supernatant was poured into a 50 ml distillation flask redesigned after Sun et al. (2001), and distilled at 110 °C for 20 min for Os. 5 ml of H_2O was used to extract the Os from a water–ice bath, and the solution was used for ICP–MS measurement of the Os isotopes.

4. Results

A total of six mica Ar–Ar ages and twenty-two molybdenite Re–Os model ages were obtained in this study. Summary of the Ar–Ar data of the biotite and muscovite from Dahutang are given in Supplementary Tables B.3-1–3-2. Plots of the $^{40}Ar/^{39}Ar$ age spectra for the Dahutang deposit are illustrated in Fig. A.2. Published and new granite ages (zircon and monazite U–Pb, mica $^{40}Ar/^{39}Ar$ dating) and molybdenite Re–Os model ages are also compiled and summarized in Supplementary Tables B.4–B.5 and illustrated in Fig. 1.

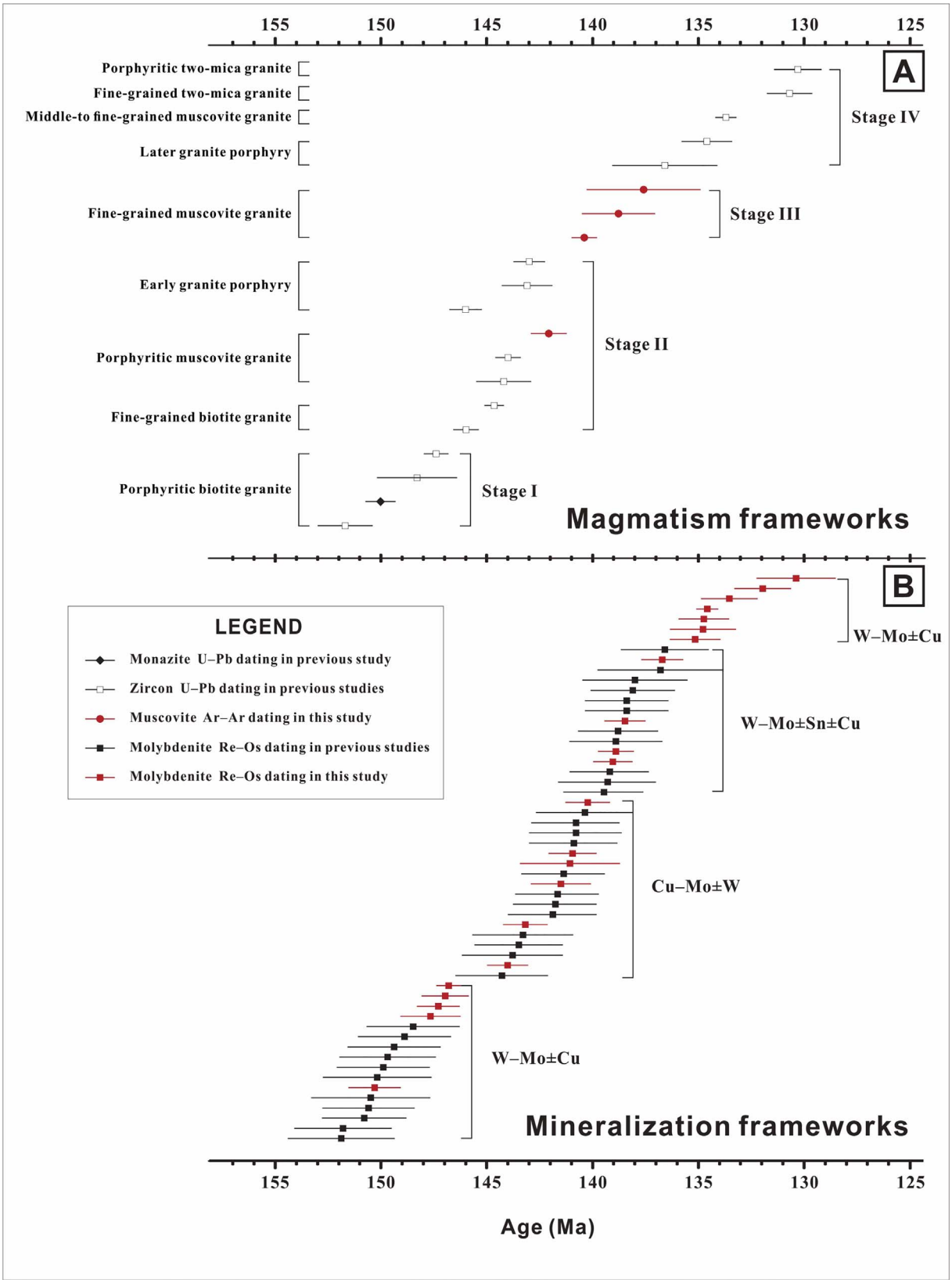

Fig. 1. Box-and-whisker plot of the magmatic and mineralization age data of the Dahutang deposit.

5. Discussion

5.1. Mesozoic magmatism and mineralization frameworks at Dahutang

As shown in Fig. 1A and B, our age data have filled some of the magmatic/mineralization age gaps, and have established a long-lived (20 m.y.) magmatism and mineralization at Dahutang. Taking the analytical uncertainties into account, our new magmatic age compilation shows that the ore-forming granites were emplaced during ca. 153.0–129.2 Ma, with one small age gap at 133.2–131.8 Ma. The mineralization ages are far more continuous than previously documented, and lasted from 154.4 to 128.5 Ma. These new and published ages, integrated with field geological and petrographic observations, indicate that the Mesozoic Dahutang magmatism and mineralization occurred in two major periods: the Late Jurassic (ca. 153–147 Ma) and the Late Jurassic to Early Cretaceous (ca. 146–130 Ma).

5.1.1. The Late Jurassic (ca. 153–147 Ma)

5.1.1.1. Stage I: W–Mo ± Cu mineralization (ca. 153–147 Ma). The porphyritic biotite granite (G1) intruded the Neoproterozoic Jiuling granodiorite batholith and Shuangqiaoshan Group in North, Central and South Dahutang and is the oldest Mesozoic granite in the area (ca. 153.0–146.8 Ma; Mao et al., 2015; Ye et al., 2016; Zhang et al., 2016). The hydrothermal biotite megacrysts sample (DH-31) from a hydrothermal breccia-type orebody in Central Dahutang yielded a well-defined plateau age of 149.2 ± 1.1 Ma, which is largely coeval with the nearby porphyritic biotite granite (zircon U–Pb age: 148.3 ± 1.9 Ma; Mao et al., 2015), suggesting that the latter may have generated the hydrothermal breccias. It is worth noting that our biotite Ar–Ar dating also yielded apparent ages of 143.9 Ma and 135.6 Ma, which may record the following Stage II and IV magmatic-hydrothermal events (to be explained later). Hence, we suggest that porphyritic biotite granite was emplaced during around 153–147 Ma, accompanied with intense hydrothermal (cryptoexplosive)-breccia-type mineralization.

Coeval with the Stage I magmatic-hydrothermal event are three molybdenite Re–Os model ages (DH-332: 147.3 ± 1.0 Ma; DH-352: 150.3 ± 1.3 Ma; DH-126: 147.7 ± 1.4 Ma) of the disseminated-/veinlet-type orebodies in North and Central Dahutang, and two molybdenite Re–Os model ages (DH-209: 146.8 ± 0.6 Ma; DH-19: 147.0 ± 1.1 Ma) of the large wolframite-bearing quartz-vein-type orebodies in North and South Dahutang. The presence of major mineralization at Dahutang during this period is also supported by six published molybdenite Re–Os model ages (ca. 148.5–151.9 Ma) in North Dahutang (Xiang et al., 2013), together with five molybdenite Re–Os model ages (ca. 148.9–150.8 Ma) in South Dahutang (Zhang et al., 2016).

Field geology and petrographic observations of samples used for Re–Os dating suggest that the mineralization in Stage I is characterized by the formation of hydrothermal breccia, disseminated/veinlet and large wolframite-bearing quartz vein type orebodies with the accompanying abundant W–Mo ± Cu mineralization, which mainly shows as wolframite – molybdenite – scheelite ± chalcopyrite mineralized breccias, scheelite – wolframite – molybdenite ± chalcopyrite – quartz disseminates/veinlets, and large wolframite – molybdenite – quartz veins. Combined with the published and new granite ages and molybdenite Re–Os ages, we suggest that the W–Mo ± Cu mineralization in Stage I is associated with the emplacement of porphyritic biotite granite during 153–147 Ma.

5.1.2. The Late Jurassic to early Cretaceous (ca. 146–130 Ma)

The Late Jurassic to Early Cretaceous period (ca. 146–130 Ma), mainly forming the Cu–Mo–W ± Sn mineralization and overprinting the W–Mo ± Cu mineralization of Stage I, can be further subdivided into three mineralization stages: Cu–Mo ± W mineralization (Stage II), W–Mo ± Sn ± Cu mineralization (Stage III) and W–Mo ± Cu mineralization (Stage IV).

5.1.2.1. Stage II: Cu–Mo ± W mineralization (ca. 146–141 Ma). Fine-grained biotite granite (G2) in North Dahutang (zircon U–Pb age: 144.7 ± 0.5 Ma, Mao et al., 2015) and Central Dahutang (zircon U–Pb age: 146.0 ± 0.6 Ma; Mao et al., 2015) are found intruding the Late Jurassic porphyritic biotite granite. Meanwhile, porphyritic muscovite granite (G3) was emplaced in Neoproterozoic Jiuling granodiorite batholith in Central Dahutang (muscovite Ar–Ar age: 142.1 ± 0.9 Ma (DH-42)) and South Dahutang (zircon U–Pb age: 144.2 ± 1.3 Ma, Huang and Jiang, 2012), but the relationships between G3 and G1, G2 are still ambiguous. Besides, at least two phases of granite porphyry intrusion were found in North and South Dahutang, with the earlier phase (G4: 143.1 ± 1.2 Ma; Mao et al., 2015) intruding the fine-grained biotite granite (G2) in North Dahutang and associated with the Cu–Mo ± W mineralization.

In this study, the two molybdenite Re–Os model ages (144.0 ± 1.0 Ma and 141.5 ± 1.4 Ma) obtained from the large wolframite-bearing quartz-vein-type orebodies in North Dahutang, one molybdenite Re–Os model age (DH-17: 141.1 ± 2.4 Ma) from the same orebody type in South Dahutang, and two molybdenite Re–Os model ages (143.2 Ma and 141.0 Ma) from the disseminated-/veinlet-type orebodies in Central and North Dahutang are generally coeval with the magmatic ages above-mentioned.

The mineralization in Stage II is characterized by the abundant Cu–Mo ± W mineralization, which mainly shows as disseminated/veinlets scheelite – molybdenite mineralization in porphyritic muscovite granite, disseminated/veinlets scheelite – molybdenite – chalcopyrite mineralization in fine-grained biotite granite, and molybdenite – chalcopyrite mineralization in early granite porphyry. Stage II mineralization also commonly overprinted the W–Mo ± Cu mineralization in Stage I, showing as chalcopyrite – molybdenite ± bornite ± arsenopyrite ± stannite polymetallic sulfide assemblages replacing the Stage I wolframite along cleavages in large wolframite-bearing quartz vein orebodies; chalcopyrite crosscutting and cementing the Stage I scheelite in disseminated-/veinlet-type orebodies. Combined with the published and new granite and molybdenite Re–Os ages, we suggest that the Cu–Mo ± W mineralization in Stage II is associated with the successively emplacement of fine-grained biotite granite, porphyritic muscovite granite, and earlier phase granite porphyry during ca. 146–141 Ma.

5.1.2.2. Stage III: W–Mo ± Sn ± Cu mineralization (ca. 141–136 Ma). The buried fine-grained muscovite granite (G5), mainly distributed beneath Central and South Dahutang, intruded into the porphyritic biotite granite (G1), fine-grained biotite granite (G2), porphyritic muscovite granite (G3) and the Neoproterozoic Jiuling granodiorite. Our new muscovite Ar–Ar dating on the fine-grained muscovite granite, including two ages from Central Dahutang (DH-02: 140.4 ± 0.6 Ma; DH-120: 138.8 ± 1.8 Ma) and one from South Dahutang (DH-94: 137.6 ± 2.7 Ma), are the first similar ages reported and have complemented the previous magmatic age gap at Dahutang.

Correspondingly, the two molybdenite Re–Os model ages (DH-108: 140.2 ± 1.1 Ma; DH-117: 136.7 ± 1.0 Ma) obtained from a disseminated-/veinlet-type orebody in Central Dahutang are broadly coeval with the fine-grained muscovite granite (muscovite Ar–Ar plateau age: 138.8 ± 1.8 Ma (DH-120)) in the same drill core (ZK510). It's worth noting that the two molybdenite samples are from the wolframite – molybdenite – scheelite ± chalcopyrite – quartz veins crosscutting the Stage I disseminated-/veinlet-type orebody (molybdenite Re–Os model age: 147.67 ± 1.44 Ma (DH-128)). Besides, two molybdenite samples from fine-grained muscovite granite yielded Re–Os model ages of 138.5 ± 1.0 Ma and 139.0 ± 1.0 Ma, which resemble the muscovite Ar–Ar age of 140.4 ± 0.6 Ma for the fine-grained muscovite granite in Central Dahutang. Moreover, we obtained two molybdenite

Re–Os model ages of 141.0 ± 1.2 Ma and 138.9 ± 0.9 Ma from the large wolframite-bearing quartz-vein-type orebodies in North Dahutang and one muscovite Ar–Ar plateau age of 138.6 ± 0.9 Ma (DH-42) from the large wolframite-bearing quartz-vein-type orebodies in South Dahutang, which are also coeval with fine-grained muscovite granite emplacement (Xiang et al., 2015).

Stage III is characterized by the W–Mo ± Sn ± Cu mineralization showing as wolframite – molybdenite – scheelite ± cassiterite ± chalcopyrite – quartz veinlets and scheelite ± chalcopyrite disseminates/veinlets in fine-grained muscovite granite. Locally, stage III wolframite – molybdenite – scheelite ± chalcopyrite – quartz veins (nearby the fine-grained muscovite granite) crosscut the Stage I disseminated-/veinlet-type orebody. Combined with the new granite Ar–Ar and molybdenite Re–Os ages, we suggest that the W–Mo ± Sn ± Cu mineralization in Stage III is associated with the emplacement of fine-grained muscovite granite during 141–136 Ma.

5.1.2.3. Stage IV: W–Mo ± Cu mineralization (ca. 136–130 Ma). Late granite porphyry (G6), mainly occurs as dykes and apophyses, intruded the porphyritic biotite granite (G1) and porphyritic muscovite granite (G3) in South Dahutang, where it crosscut some large quartz veins and intruded into some orebodies, but the relationships between G6 and G4, G5 are not clear. Late granite porphyry samples were dated by zircon U–Pb method to be 134.6 ± 1.2 Ma (Huang and Jiang, 2013) and 136.6 ± 2.5 Ma (Zhang et al., 2016) in South Dahutang. In addition, medium- to fine-grained muscovite granite (G7), porphyritic two-mica granite (G8) and fine-grained two-mica granite (G9) intruding the Neoproterozoic biotite granodiorite and porphyritic biotite granite (G1), have zircon U–Pb ages of 133.7 ± 0.5 Ma, 130.3 ± 1.1 Ma and 130.7 ± 1.1 Ma, respectively (Huang and Jiang, 2014). These granites were occasionally encountered in drill cores from several hundreds of meters below the surface, so the contact relationships among the G6, G7, G8, G9 are still not clear, which could be associated with the weak mineralization at ca. 136–130 Ma.

Five molybdenite Re–Os model ages from the large wolframite-bearing quartz-vein-type orebodies in South Dahutang show similar age range with Stage IV magmatism, among which three ages (134.6 ± 1.2 Ma, 135.2 ± 1.2 Ma and 134.8 ± 1.2 Ma) are coeval with the zircon U–Pb age of 134.6 ± 1.2 Ma for late granite porphyry in South Dahutang (Huang and Jiang, 2013). Two ages (132.0 ± 1.3 Ma and 130.4 ± 1.9 Ma) are coeval with the porphyritic two-mica granite (zircon U–Pb age: 130.3 ± 1.1 Ma) and fine-grained two-mica granite (130.7 ± 1.1 Ma) (Huang and Jiang, 2013). Besides, the two molybdenite Re–Os model ages of 134.6 ± 0.5 Ma and 133.5 ± 1.4 Ma obtained from disseminated-/veinlet-type orebodies in Central Dahutang are similar to the ages of medium- to fine-grained muscovite granite (zircon U–Pb age: 133.7 ± 0.5 Ma) (Huang and Jiang, 2013).

Stage IV is characterized by the weak W–Mo ± Cu mineralization commonly overprinting the early-stage mineralization, which mainly shows as molybdenite ± chalcopyrite mineralization along the fractures in quartz vein walls and the scheelite ± chalcopyrite veinlets crosscutting the large wolframite-bearing quartz veins. Combined with the published and new granite and molybdenite Re–Os ages, we suggest that the last weak W–Mo ± Cu mineralization in Stage IV may associate with the last magmatism during 136–130 Ma.

5.2. Relationship between granite evolution and mineralization process

As we discussed above, nine types of Late Mesozoic granites exist in the Dahutang deposit, granite evolution and mineralization process are very complex. Three types of mineralization in Dahutang W–Cu–Mo deposit include disseminated/veinlets type, large wolframite-bearing-quartz veins type, and hydrothermal breccias type. However, our new research finds that there is no discernible spatial or temporal relationships among the three types of mineralization. These different mineralization styles commonly coexist and mutually overprint.

Disseminated/veinlet type: Taking No.1 ore belt ZK510 drill core in Central Dahutang as an example. We obtained three molybdenite Re–Os model ages (147.7 Ma, 140.2 Ma, and 136.7 Ma) from the drill core ZK510, which suggest that the oldest Re-Os age (147.7 Ma) is coeval with the porphyritic biotite granite (zircon U–Pb age: 148.3 ± 1.9 Ma; Mao et al., 2015), the other two ages (140.2 Ma and 136.7 Ma) are coeval with the fine-grained muscovite granite (muscovite Ar–Ar plateau age: 138.8 ± 1.8 Ma) in the same drill core (ZK510).

Hydrothermal breccia type: Taking Xidouya hydrothermal breccias type ore body in Central Dahutang as an example. The hydrothermal biotite megacrysts sample from hydrothermal breccias yielded a well-defined plateau age of 149.2 ± 1.1 Ma, which is largely coeval with the nearby porphyritic biotite granite (zircon U–Pb age: 148.3 ± 1.9 Ma; Mao et al., 2015). Our biotite Ar–Ar dating also yielded apparent ages of 143.9 Ma and 135.6 Ma, which may record the following Stage II and IV magmatic-hydrothermal events.

Large wolframite-bearing-quartz vein type: Taking Shiweidong No. 38 large wolframite- bearing- quartz vein in South Dahutang as an example. We also obtained three molybdenite Re–Os model ages (147.0 Ma, 141.0 Ma, and 132.0 Ma) from the No.38 large wolframite-bearing- quartz vein, which suggest that the oldest Re-Os age (147.0 Ma) is coeval with the porphyritic biotite granite, the other two ages are coeval with the muscovite granite.

Above all, obviously, all three types of mineralization began to form during the early granite intrusion in Dahutang. With the continuous intrusion of the later stage granites, three types of mineralization were successively forming and superimposed. Therefore, we suggest that nine types of granites were emplaced in the Dahutang area over a long and multiphase magmatism (ca. 152–130 Ma). The complex Dahutang W–Cu–Mo polymetallic mineralization related to this multiphase magmatism also lasted for around 20 m.y. and displays multiphase characteristics. The long-lived multiphase mineralization leads to a very complex interspersed and superimposed relationships between ore minerals and granite rocks. Although it is difficult to correlate each phase mineralization to each magmatic phase, the mineralization ages are generally consistent with the magmatic ages.

5.3. Ore genesis model of the Dahutang deposit

In summary, we propose the following ore genesis evolutionary model for the Dahutang deposit (Fig. 2), mainly based on our new age constrains and previous studies:

In stage I (ca. 153–147 Ma), porphyritic biotite granite stocks were emplaced at Dahutang. The magmatic-hydrothermal fluids of these intrusions may have converged onto the apical parts and led to cryptoexplosions that formed hydrothermal breccia-type orebodies. The large wolframite-bearing quartz-vein-type orebodies were likely formed when the magmatic-hydrothermal fluids ascended along the fault system. The ore-forming fluids that entered the Jiuling Neoproterozoic biotite granodiorite batholith generated intense greisenization and the disseminated-/veinlet-type orebodies. In stage II (ca. 146–141 Ma), the Cu–Mo mineralization overprinted on the early-stage W-dominated mineralization, along with the emplacements of fine-grained biotite granite, early granite porphyry and porphyritic muscovite granite in North and Central Dahutang. In stage III (ca. 141–136 Ma), the fine-grained muscovite granite was emplaced with the moderate W–Mo ± Sn ± Cu mineralization, which locally overprinted the Stage I and II mineralization. In stage IV (ca. 136–130 Ma), the late granite porphyry, medium- to fine-grained muscovite granite, porphyritic two-mica granite, and fine-grained two-mica granite dykes successively emplaced into the early phase granites and orebodies. Weak W–Mo ± Cu mineralization occurred and overprinted/reworked the previous mineralization.

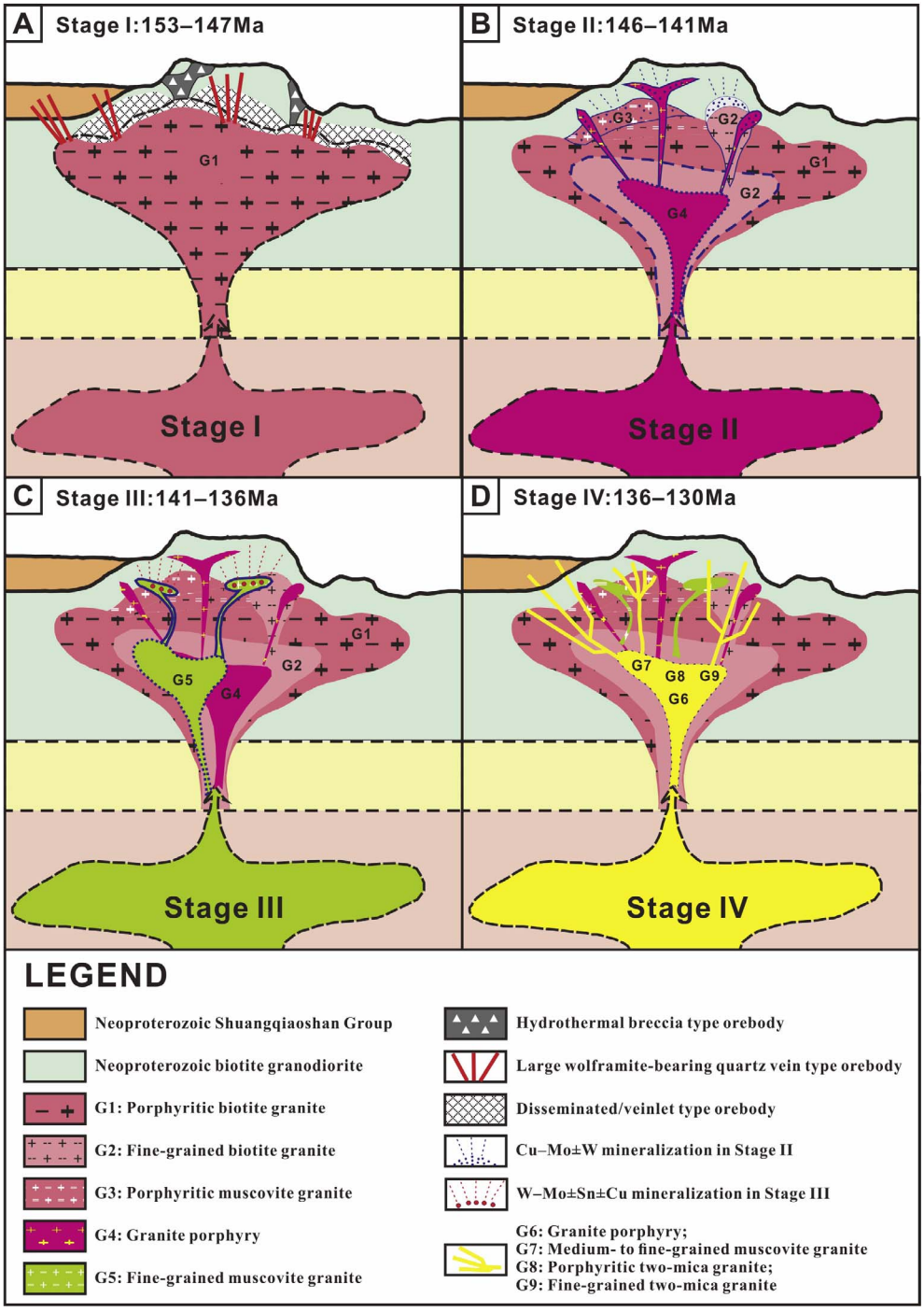

Fig. 2. Schematic magmatic and ore genesis model of the Dahutang deposit.

6. Conclusions

Our geochronological study indicates that the giant Dahutang W–Cu–Mo deposit was formed by a long-lived (20 m.y.) and multistage mineralization processes, led by a prolonged and coeval multiphase magmatism. Hence, we suggest that multiphase magmatism and continuous accumulation of mineralization play a significant role in the formation of giant Dahutang W–Cu–Mo deposit.

Acknowledgements

This study was financially supported by the DREAM project of MOST China (2016YFC0600405), the National Natural Science Foundation of China (Nos. 41672079, 41372085) and the Strategic Priority Research Program (B) of Chinese Academy of Sciences (No. XDB18000000). Drs. Chanchan Zhang, Yang Yu and Jie Li are thanked for their help in the field work. We are grateful to Mr. Gangle Zhan, Mr. Quanshi Zuo, and the staffs from the Jiangxi BGMR for the field assistance and fruitful discussion. We also thank a number of technical staff for assistance during this study, especially Shengling Sun for assistance during molybdenite Re–Os isotopic dating; Jing Zhou for assistance during mica Ar–Ar dating. This is contribution No. IS-2512 from GIGCAS.

Appendix A. Supplementary data

Supplementary data associated with this article can be found, in the online version, at http://dx.doi.org/10.1016/j.oregeorev.2018.02.033.

References

Buret, Y., Quadt, A.V., Heinrich, C., Selby, D., Wälle, M., Peytcheva, I., 2016. From a long-lived upper-crustal magma chamber to rapid porphyry copper emplacement: reading the geochemistry of zircon crystals at Bajo de la Alumbrera (NW Argentina). Earth Planet. Sci. Lett. 450, 120–131.

Cathles, L.M., Erendi, A.H.J., Barrie, T., 1997. How long can a hydrothermal system be sustained by a single intrusive event. Econ. Geol. 92, 766–771.

Feng, C.Y., Zhang, D.Q., Xiang, X.K., Li, D.X., Qu, H.Y., Liu, J.N., Xiao, Y., 2012. Re-Os isotopic dating of molybdenite from the Dahutang tungsten deposit in northwestern Jiangxi Province and its geological implication. Acta Petrol. Sin. 28, 3858–3868 (in Chinese with English abstract).

Hsu, K.C., 1943. Tungsten deposits of southern Kiangsi China. Econ. Geol. 38, 431–474.

Huang, L.C., Jiang, S.Y., 2012. Zircon U-Pb geochronology, geochemistry and petrogenesis of the porphyry-like muscovite granite in the Dahutang tungsten deposit Jiangxi Province. Acta Petrol. Sin. 28, 3887–3900 (in Chinese with English abstract).

Huang, L.C., Jiang, S.Y., 2013. Geochronology, geochemistry and petrogenesis of the tungsten-bearing porphyritic granite in the Dahutang tungsten deposit Jiangxi Province. Acta Petrol. Sin. 28, 4323–4335 (in Chinese with English abstract).

Huang, L.C., Jiang, S.Y., 2014. Highly-fractionated S-type granites from the giant Dahutang tungsten deposit in Jiangnan Orogen, Southeast China: geochronology, petrogenesis and their relationship with W mineralization. Lithos 202–203, 207–226.

Jiang, S.Y., Peng, N.J., Huang, L.C., Xu, Y.M., Zhan, G.L., Dan, X.H., 2015. Geological characteristic and ore genesis of the giant tungsten deposits from the Dahutang ore-concentrated district in northern Jiangxi Province. Acta Petrol. Sin. 31, 639–655 (in Chinese with English abstract).

Jourdan, F., Renne, P.R., 2007. Age calibration of the Fish Canyon sanidine 40 Ar/39 Ar dating standard using primary K-Ar standards. Geochim. Cosmochim. Acta 71, 387–402.

Leng, C.B., Zhang, X.C., Hu, R.Z., Wang, S.X., Zhong, H., Wang, W.Q., Bi, X.W., 2012. Zircon U-Pb and molybdenite Re–Os geochronology and Sr–Nd–Pb–Hf isotopic constraints on the genesis of the Xuejiping porphyry copper deposit in Zhongdian, Northwest Yunnan China. J. Asian Earth Sci. 60, 31–48.

Li, N., Chen, Y.J., Santosh, M., Yao, J.M., Li, J., 2011. The 1.85 Ga Mo mineralization in the Xiong'er Terrane, China: implications for metallogeny associated with assembly of the Columbia supercontinent. Precambr. Res. 186, 220–232.

Li, X.H., Li, Z.X., Ge, W.C., Zhou, H.W., Li, W.X., Liu, Y., Wingate, M.T.D., 2003. Neoproterozoic granitoids in South China: crustal melting above a mantle plume at ca. 825 Ma? Precambr. Res. 122, 45–83.

Ludwig, K.R., 2003. User's Manual for Isoplot 3.0: A Geochronological Toolkit for Microsoft Excel. Berkeley Geochronology Center, Berkeley, CA.

Mao, Z.H., Cheng, Y.B., Liu, J.J., Yuan, S.D., Wu, S.H., Xiang, X.K., Luo, X.H., 2013. Geology and molybdenite Re–Os age of the Dahutang granite-related veinlets-disseminated tungsten ore field in the Jiangxi Province China. Ore Geol. Rev. 53, 422–433.

Mao, Z.H., Liu, J.J., Mao, J.W., Deng, J., Zhang, F., Meng, X.Y., Xiong, B.K., Xiang, X.K., Luo, X.H., 2015. Geochronology and geochemistry of granitoids related to the giant Dahutang tungsten deposit, Middle Yangtze River region, China: implications for petrogenesis, geodynamic setting, and mineralization. Gondwana Res. 28, 816–836.

Mercer, C.N., Reed, M.H., Mercer, C.M., 2015. Time scales of porphyry Cu deposit formation: insights from titanium diffusion in quartz. Econ. Geol. 110, 587–602.

Merle, R., Jourdan, F., Marzoli, A., Renne, P., Grange, M., Girardeau, J., 2009. Evidence of multi-phase cretaceous to quaternary alkaline magmatism on tore-madeira rise and neighboring seamounts from $^{40}Ar/^{39}Ar$ ages. J. Geol. Soc. 166, 879–894.

Northwestern Geological Team, Jiangxi Bureau of Geology, Mineral Resources, Exploration and Development, 2012. The Exploration Report of the Shiweidong, South Portion of the Dahutang Tungsten Deposit, Wuning County, Jiangxi Province. Jiangxi Jutong Mining Corporation (108pp.).

Rezeau, H., Moritz, R., Wotzlaw, J., Tayan, R., Melkonyan, R., Ulianov, A., Selby, D., Abzac, F.X., Stern, R.A., 2016. Temporal and genetic link between incremental pluton assembly and pulsed porphyry Cu-Mo formation in accretionary orogens. Geology 44, 627–630.

Shen, J.F., Chen, Z.H., Liu, L.J., Ying, L.J., Huang, F., Wang, D.H., Wang, J.H., Zeng, L., 2015. Outline of metallogeny of tungsten deposits in China. Acta Geol. Sin. 89, 1038–1050 (in Chinese with English abstract).

Sun, Y.L., Xu, P., Li, J., He, K., Chu, Z.Y., Wang, C.Y., 2010. A practical method for determination of molybdenite Re–Os age by inductively coupled plasma-mass spectrometry combined with Carius tube-HNO_3 digestion. Anal. Methods 2, 575–581.

Sun, Y.L., Zhou, M.F., Sun, M., 2001. Routine Os analysis by isotope dilution inductively coupled plasma mass spectrometry: OsO_4 in water solution gives high sensitivity. J. Anal. At. Spectrom. 26, 345–349.

U.S. Geological Survey, 2017. Mineral Commodity Summaries 2017. https://doi.org/10.3133/701 80197.

Xiang, X.K., Chen, M.S., Zhan, G.N., Qian, Z.Y., Li, H., Xu, J.H., 2012. Metallogenic geological conditions of Shimensi tungsten-polymetallic deposit in north Jiangxi Province. Contr. Geol. Miner. Resour. Res. 27, 143–155 (in Chinese with English abstract).

Xiang, X.K., Wang, P., Sun, D.M., Zhong, B., 2013. Re-Os isotopic age of molybdenite from the Shimensi tungsten polymetallic deposit in northern Jiangxi Province and its geological implications. Geol. Bull. China 32, 1824–1831 (in Chinese with English abstract).

Xiang, X.K., Yin, Q.Q., Sun, K.K., Chen, B., 2015. Origin of Dahutang syn-collisional granite porphyry in the middle segment of the Jiangnan orogen: Zircon U-Pb geochronologic, geochemical and Nd-Hf isotopic constraints. Acta. Petrol. Mineral. 34, 581–600 (in Chinese with English abstract).

Ye, H.M., Zhang, X., Zhu, Y.H., 2016. In-situ monazite U-Pb geochronology of granites in Shimensi tungsten polymetallic deposit, Jiangxi province and its geological significance. Geotect. Metal. 40, 58–70 (in Chinese with English abstract).

Zhang, M.Y., Feng, C.Y., Li, D.X., Wang, H., Zhou, J.H., Ye, S.Z., Wang, G.H., 2016. Geochronological study of the Kunshan W–Mo–Cu deposit in the Dahutang area, northern Jiangxi province and its geological significance. Geotect. Metal. 40, 503–516 (in Chinese with English abstract).

Zhang, Y., Pan, J.Y., Ma, D.S., Dan, X.H., Zhang, L.L., Xu, G.H., Yang, C.P., Jiang, Q.X., Jiang, C.Q., 2017. Re-Os molybdenite age of Dawutang tungsten ore district of northwest Jiangxi and its geological significance. Miner. Depos. 36, 749–769 (in Chinese with English abstract).

Zhang, Z.H., Geng, L., Jia, W.B., Gong, X.D., Du, Z.Z., Zhang, M.C., 2014. Regional geological characteristics study of tungsten-polymetallic ore field in Datanghu tungsten polymetallic deposit in north of Jiangxi. Chin. Min. Maga. 23, 133–148 (in Chinese with English abstract).